Interactions of Porphyrinyl-Nucleosides with DNA Using the Example of Porphyrinyl-Thymidine

Vinay Wandrekar, William R. Trumble [a] and Leszek Czuchajowski*

Department of Chemistry and Department of Microbiology, Molecular Biology and Biochemistry [a], University of Idaho, Moscow, ID 83844-2343 USA

Received October 27, 1995

meso-Tri(*N*-methyl-4-pyridinium)porphyrinyl-*p*-phenylene-5'-*O*-thymidine, interacting with plasmid ds DNA showed an 8 nm red-shift of the Soret band. The observed Soret band shift was 4 nm less than the shift of the respective *meso*-tetra(*N*-methyl-4-pyridinium)porphyrin, which is usually assumed to indicate intercalation. Experimental spectra and the MMX- and AM-1 calculations of a series of model structures further suggest that the investigated porphyrinyl-thymidine also interacts with adenine due to its nucleobase. The possibility of intercalation was also viewed based on interaction of immobilized porphyrin with ds DNA. Theoretical considerations suggested that there are no steric limitations to the formation of a system in which the porphyrinyl-thymidine in question interacts with a molecule of porphyrinyl-adenosine, *via* A-T base pairing, to join two ds DNA molecules.

J. Heterocyclic Chem., **33**, 1775 (1996).

The porphyrinyl-nucleosides, representing a new class of compounds, were synthesized in this laboratory and have been previously described in this Journal [1]. We were interested in evaluating 1) the involvement of the cationic porphyrin structural unit of these compounds in interaction with DNA (do they intercalate or bind electrostatically?) and 2) the involvement of their nucleoside base structure in interactions with a complementary nucleobase (Could one expect to join two DNA molecules by a porphyrin-nucleoside(1)···nucleoside(2)-porphyrin system?). Both experimental and theoretical results from our evaluations are described in this article.

Attention was focused primarily on *meso*-tri(*M*-methyl-4-pyridinium)porphyrinyl-*p*-phenylene-5'-*O*-thymidine (denoted further as PT or P-phen-T, Figure 1) as an important representative of porphyrinyl-nucleosides, and secondarily on the corresponding porphyrinyl-adenosine (PA or P-phen-A) with which the formation of a DNA-P-phen-T···A-phen-P-DNA system could be investigated. First, using molecular mechanics calculations [2] and the semi-empirical AM-1 quantum chemical method [3], the conformation and energetic preferences of the phen-T and phen-A structural fragments were calculated and the preferred conformer utilized in modeling of the P-phen-T···A-phen-P putative double intercalator. From its 3-D structure one could deduct its steric preferences and limitations concerning formation of the DNA-P-phen-T···A-phen-P-DNA system. Second, the possibility of an interaction of P-phen-T with DNA was approached both experimentally and theoretically based on the changes of its electronic structure as measured by uv-vis absorption spectra of the interacting system. For some calculations a set of reasonably simplified models were evaluated. Third, the spectra of the components of the porphyrinyl-*p*-phenylene-nucleoside, exemplified by P-phen-T and P-phen-A, were examined to determine the influence of stepwise joining of the structural fragments involved. The experimental data dealing with the interaction of ds DNA with porphyrin, DNA with P-phen-T and DNA-P-phen-T···A were supplemented by the results of the interaction with DNA using an immobilized porphyrin. Moreover, it has been shown that the most characteristic region of porphyrin absorption, *i.e.* the Soret band region, is influenced not only by interactions with DNA but also by the attachment of different type of nucleosides to the porphyrin core.

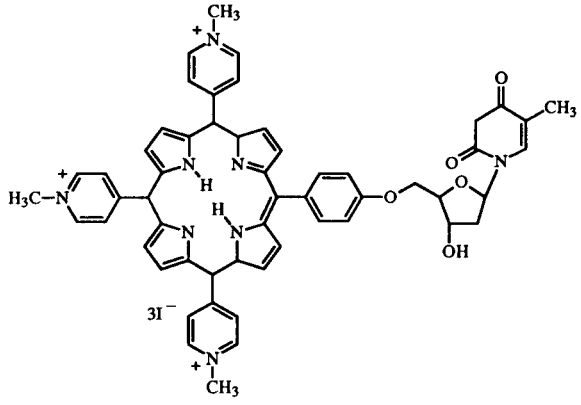

Figrue 1. *meso*-Tri(*N*-methyl-4-pyridinium)porphyrinyl-*p*-phenylene-5'-*O*-thymidine **2**.

Results.

Phenyl-5'-*O*-thymidine and phenyl-5'-*O*- adenosine represent important structural components of the P-phen-T and P-phen-A system. The 3-D structure of these compounds is of real interest. Their conformational states were calculated as described in the Theoretical section, using atom numbering as shown in Figure 2. The results of MMX calculations (see Theoretical) were taken directly from energy surfaces (not shown) and after full optimization, the steric energies were calculated for 7 conformers of phen-T and 6 conformers of phen-A, all representing strainless structures. The respective heats of formation (which consider the conjugation effects)

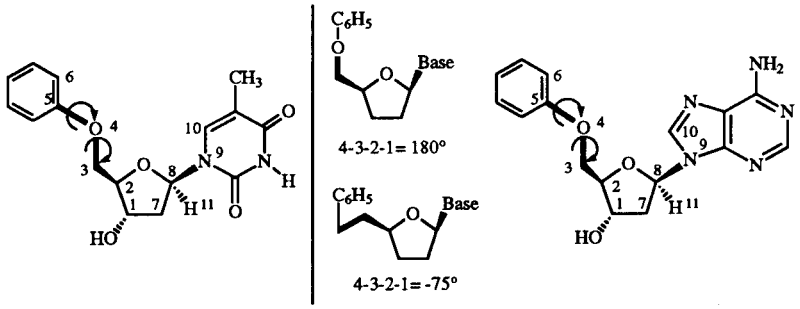

Figure 2. Phenyl-5'-*O*-thymidine (left) and phenyl-5'-*O*-adenosine (right) as models for conformational analysis. Carbons C(10) are fixed over furanose rings, carbons C(7) are fixed in the "up" conformation, the OH group orientation is assumed unimportant.

were calculated by the AM-1 method. The most characteristic conformers are shown in Figures 3 and 4, while the calculated values are summarized in Table 1. The MMX energies are in the range of 10.97 to 12.68

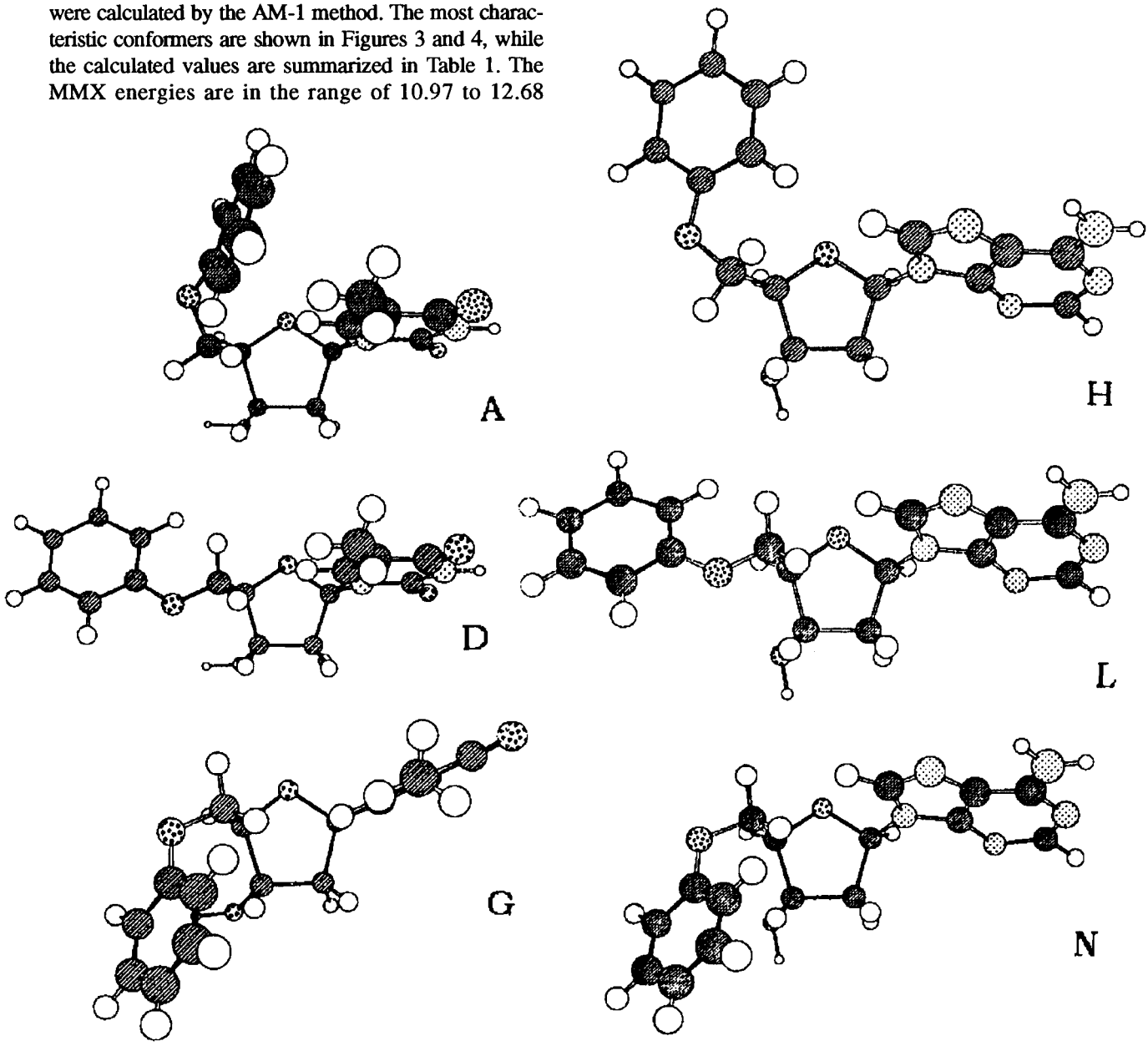

Figure 3. Optimized (by MMX method) conformers of phenyl-5'-*O*-thymidine (see also Figure 2 and Table 1).

Figure 4. Optimized (by MMX method) conformers of phenyl-5'-*O*-adenosine (see also Figure 2 and Table 1).

Table 1

Molecular Mechanics Energy and AM-1 Heats of Formation of the Optimized Conformers of Phenyl-5'-*O*-thymidine (Conformers A through G) and phenyl-5'-*O*-adenosine (Conformers H through N), see Figures 3 and 4

Structure	After Full MMX Optimization				After AM1 Optimization			
	MMX Energy (Kcal/mol)	Torsional Angles (°) 6-5-4-3	5-4-3-2	4-3-2-1	AM1 Hf (Kcal/mol)	Torisonal Angles (°) 6-5-4-3	5-4-3-2	4-3-2-1
A	11.28	-27.31	-73.48	-177.86	-146.51	-54.87	-101.21	-172.62
B	11.48	0.74	179.62	-176.05	-147.38	-3.15	-178.58	-173.63
C	12.02	11.01	72.17	170.10	-146.76	9.61	72.82	-172.64
D	11.03	-16.80	-68.66	-65.07	-149.45	4.28	-82.34	-68.15
E	11.26	-9.36	-73.44	-70.10	-149.34	5.31	-83.16	-69.20
F	10.97	-7.47	-175.90	-67.23	-148.74	-3.64	-175.54	-66.80
G	12.68	42.98	75.49	-73.65	-147.87	56.42	91.43	-74.27
H	38.47	-19.44	-76.14	-178.41	-0.18	-7.92	-78.11	-138.39
I	38.25	-0.03	179.07	-176.23	-1.65	-0.36	178.78	-175.92
K	38.62	14.67	69.84	-177.79	-1.21	-1.18	74.28	-149.41
L	38.67	-11.44	-72.33	-67.30	-2.31	-2.09	-78.00	-67.06
M	38.42	-4.41	-176.97	-64.96	-0.78	-6.75	-174.66	-61.35
N	40.04	44.06	76.97	-69.88	-0.93	48.50	87.66	-74.33

kcal/mol for phen-T and 38.25 to 40.04 for phen-A, demonstrating that the differences in energy are small, with values of 1.71 and 2.59 kcal/mol, respectively. Differences in heats of formation are similarly small, -149.45 to -146.51 and -2.31 to -0.18 kcal/mol, for phen-T and phen-A, respectively; note, however, that the lowest steric energy values do not necessarily correspond to the lowest values of heats of formation. The phen-T and phen-A conformers of lowest heats of formation (D and L, respectively, see Figures 3 and 4) were selected to be connected with the *meso*-center of the porphine core at an angle of 90°. The thymine and adenine nucleobases of the resulting structures were paired by H-bonds in a manner typical for T···A pairs in DNA (N-H-O and N-H-N distances fixed at 2.1Å and 3.3Å, respectively [4]. The resulting P-phen-T···A-phen-P system, see Figure 5, is shown in top and side views in Figure 6.

two double strands of the intercalated DNA molecules can not assume parallel positions; however, considering the flexibility of each ds DNA chain and the low steric energy barriers characterizing the conformational states of the phenylene-nucleosidic furanose ring structural units, no steric objections to the formation of a double intercalated system, DNA-PT···AP···DNA should be expected. Two, the external (non-intercalating) interactions between the cationic porphyrin centers and the negative phosphate groups of DNA [5], for which steric requirements are much more limited than for intercalation, could be seriously considered as an alternative or strongly competitive type of interaction.

It has generally been accepted [6] that a red-shift of 12 nm (from the starting position in the 400-428 nm range) of the Soret band of porphyrin interacting with ds DNA, is a proof of intercalation. Before approaching this prob-

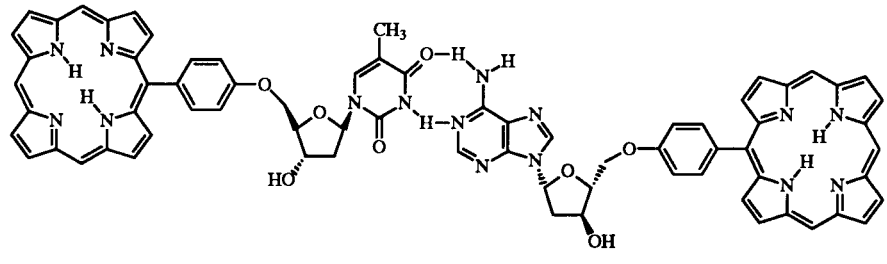

Figure 5. A porphyrinyl-*p*-phenylene-thymidine...adenosine-*p*-phenylene-porphyrinyl dimer (qPT•••AqP) (see also Figure 6 for calculated 3-D structure).

When compared to synthetic porphyrinyl-thymidine and porphyrinyl-adenosine, the P-phen-T···A-phen-P dimer is simplified only by the absence of three *meso*-*N*-methylpyridinium substituents attached to each porphine unit. If one assumes intercalation into different ds DNA molecules (between two G···C pairs) by each of these two porphine units, one can postulate the following possibilities: one, the

lem it seemed reasonable to determine what is the influence on the position of this band, and other visible region bands, of the structural units attached to porphine core in a porphyrinyl-nucleoside, exemplified in our studies by porphyrinyl-*p*-phenylene-thymidine. We have found that, with regard to the Soret band, there is no consistency in changes of its position in dependence of the number of the

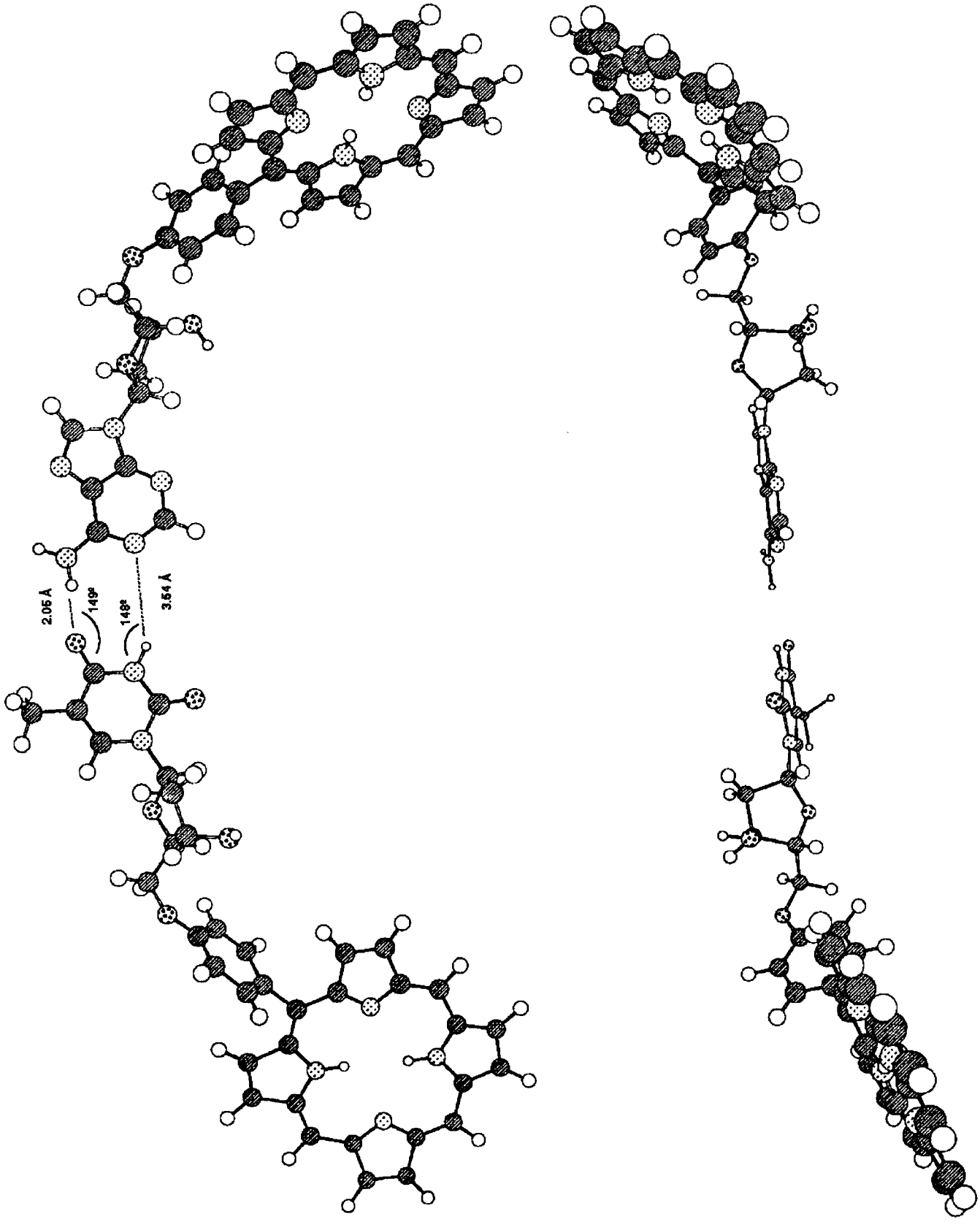

Figure 6. The top view (upper) and side view (lower) of the optimized qPT•••AqP dimer shown in Figure 5.

p-phenylene-nucleoside units attached either to *meso*-pyridylporphine or to *meso*-(*N*-methylpridinium)porphine. The experimental Soret band values for the former system with the attachment of one, two or three *p*-phenylene-thymidine units are 418, 418 and 427 nm, respectively; for the attachment of one, two or four (protected) uridine units the values are 427, 427 and 418 nm, while in the case of the attachment of four *p*-phenylene-adenosine units [1] the value is 424.5 nm. However, the remaining pyridine **I-IV** bands in the visible region all show red-shifts increasing with the number of *p*-phenylene-thymidine units attached: IV band 514 → 516 → 521; III band 549 → 553 → 560 nm; II band 588 → 591 → 595 nm; I band 644 → 648 → 651 nm. Also, the general band intensity pattern changes from the typical "ethio" type to a new one which is different from all four patterns known for porphyrins, Figure 7.

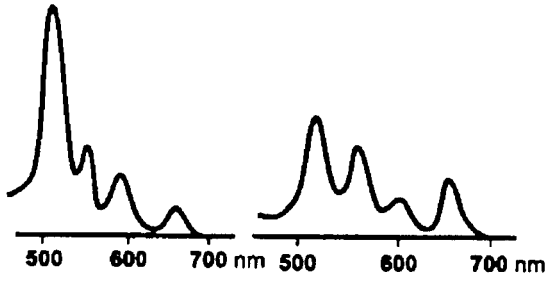

Figure 7. Visible absoption spectra characteristic for ethio-type prophyrins (left) and some porphyrinyl-nucleosides (right).

Considering only porphyrinyl-thymidine, PT, we have observed that interaction with ds DNA red-shifts the Soret band by 8 nm as compared to the 12 nm shift characteristic for *meso*-tetra(*N*-methyl-4-pyridinium)porphyrin (*i.e.* the corresponding porphyrin in which the nucleoside substituents is absent).

Since it was necessary to look at the results of calculations of the uv-vis absorption spectra of the structures in question, this was done by considering five models, shown in Figure 8, of gradually increasing complexity. The simplest one has one pyridyl ring (or alternatively pyridinium ring obtained by protonation of the N center) attached in a *meso*-position to porphine core, the resulting structure being either angled (70°) or coplanar. In other models, thimine is attached as the second *meso*-substituent either directly or *via* a *p*-phenylene bridge or is attached as a thymidine nucleoside by the same bridge structure. As shown in Table 2, the Soret band appears in the 355-340 nm range, it is about 40 nm below the experimental value for the porphine core alone (395 nm in benzene, 385 as vapor). This discrepancy should be attributed to the semiempirical method (AM-1) applied in the calculations instead of an *ab initio* approach. It is similar to differences between the calculated and experimental Soret positions for porphyrins substituted by other substituents

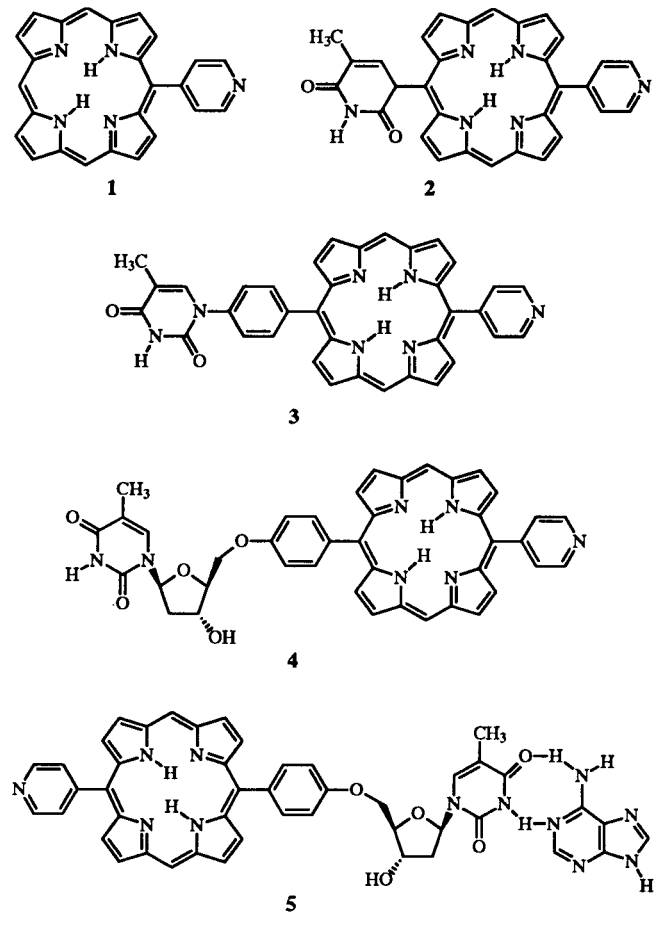

Figure 8. Set of models for which uv-vis absorption spectra were calculated (by AM-1 method).

Table 2

Calculated Absorption Maxima of Model Substances Shown in Figure 8 and Experimental Maxima for the Investigated Systems in the Soret Band Region

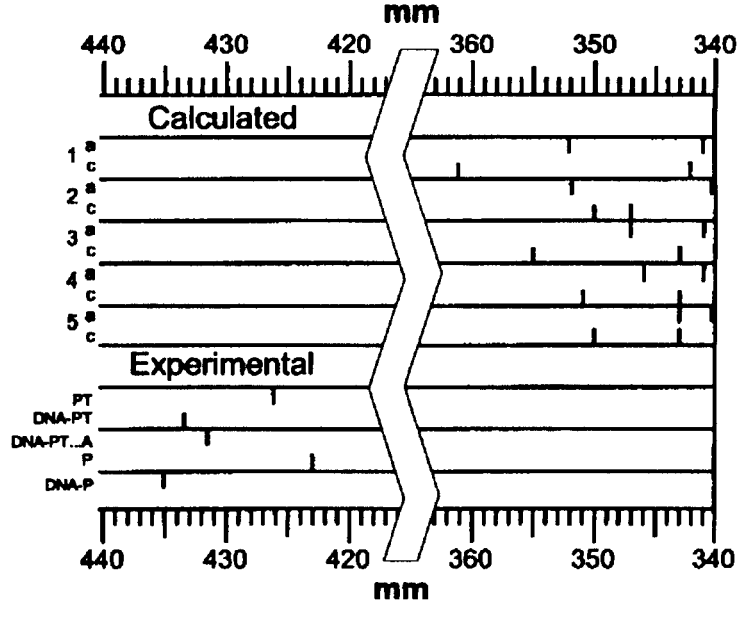

than nucleosides (*e.g.*, *meso*-tetraphenylporphyrin, 372 (2.01) and 361 (3.15) *vs* 419 (2.63) or *meso*-[2.2]paracyclophanyl-triphenylporphyrin, 394 (0.88), 364 (1.27) and 386 (1.35), 375 (1.42) *vs* 424 (2.24), the values in brackets giving oscillator strength (all calculations by CNDO/S)) [7]. Still, an interesting observation was noted. When pyridyl-attached to the porphine core was coplanar with porphine and not angled (at 70°), the intensity of the longer wave theoretical Soret band component was always higher (by 10-49%) for the considered models (1,2,3, Figure 8). Only after the quasi-PT model (qPT, **4**) was attached to A, (q-PT···A), (**5**, Figures 8 and 9) the intensities became virtually equal. The same trend of changes was revealed by the respective models in which the N center of the pyridine ring was not neutral but pyridinium H-N+, more like that in the applied *N*-methylpyridinium substituents. In such a case the Soret band was calculated at 467 nm (oscillator strength 0.97) for the angled structure and 401 nm (1.26) for coplanar; intensity of the Soret band for the coplanar arrangement was again greater (here by 30%) than for the angled arrangement. This might have some conceptual implications. When a cationic porphyrin interacts with DNA (by a reaction that has historically been assumed to be intercalation), not only does a red-shift of the Soret band appear (by >10 nm) but a decrease in intensity of this band occurs. The intercalation phenomenon would need, however, for the pyridinium ring to be coplanar with the porphyrin core in order to allow successful intercalation. The resulting intensity change of the Soret band should correspond, according to calculations, to an increase of the intensity which is opposite to what experimental spectra show. This discrepancy could support recent objections of Monaco and Zhao [8] against intercalation.

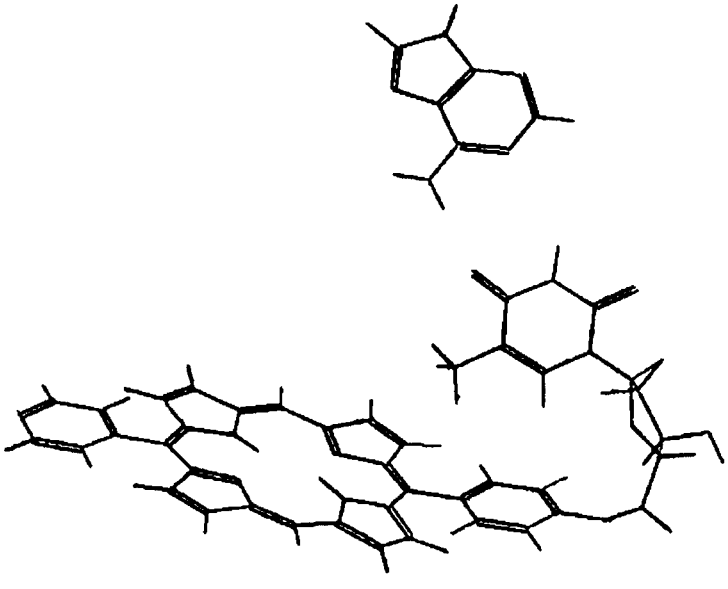

Figure 9. One of the conformers of pyridyl-porphyrinyl-5'-*O*-thymidine interacting with adenine (model **5** in Figure 8).

This also seems to be supported by the model structure **4** (denoted as quasi-porphyrinyl-thymidine, qPT) when it was involved, as a conformer shown in Figure 9, in the process of T···A pairing with the adenine nucleobase. For the theoretical system in its angled (pyridine *vs* porphine) form, blue shifts of the theoretical Soret band (346 → 343 nm and 341 → 340 nm) were calculated, while for the coplanar form there was no shift (351 *vs* 351 nm, and 343 *vs* 343 nm) predicted. Characteristically, the Soret band in the experimental spectra of the synthesized porphyrinyl-thymidine which was interacted with DNA, showed a blue-shift when it interacted with adenine, DNA-PT···A, (435 → 431.5 nm), similar to the shift calculated for the angled but not coplanar qPT.

Table 3

Calculated Absorption Maxima of Model Substances Shown in Figure 8 and Experimental Maxima for the Investigated Systems in the200-270 nm Region

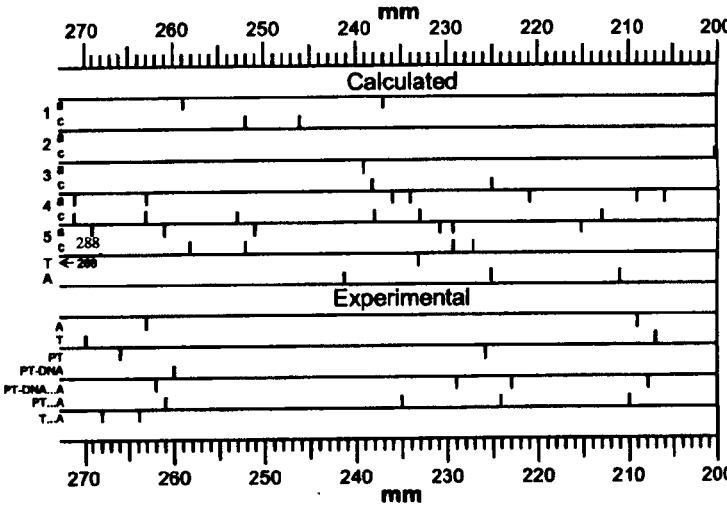

The absorption characteristic for nucleosides appears below 280 nm. It was, therefore, interesting to look at this region in the calculated spectra of the model structures **1-4** and to compare them with the experimental values of the synthesized compounds, see Table 3. Attachment of thymine nucleobase in the form of thymidine to *meso*-tri(*N*-methylpyridinium)porphyrin *via* a *p*-phenylene bridge caused a blue-shift in the experimental spectra from 270 nm to 266 nm; H-bonding with adenine (absorption at 263 nm) resulted in a further blue-shift to 261 nm. Theoretical calculations reveal the same trend, 288 → 271 (**4**) → 269/8 (**5**) nm. The interaction of PT with DNA, (DNA-PT), shifts the absorption maximum of PT from 266 (visible as a shoulder) to 260 nm (Figure 10), which is of the same energy as that calculated for qPT interacting with adenine, (**5**), (qPT···A). Further interaction with A (represented by DNA-PT···A system) does not cause any visible spectral changes, perhaps because - as calculations show - the *ca* 260 nm energy value is the limit of the maximum shift originating from thymine, caused by interaction with adenine. However, in this regard some new

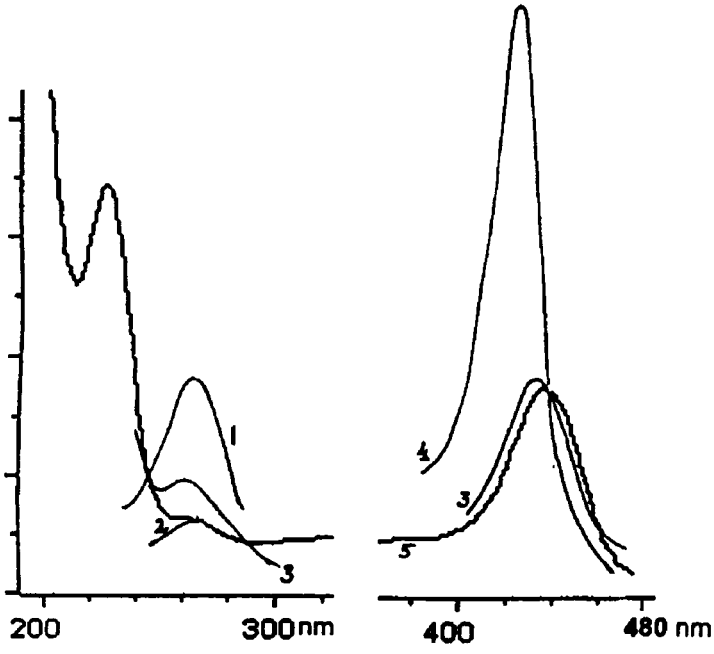

Figure 10. Experimental uv-vis absorption spectra in the 200-280 nm region (left) and 380-460 nm region (right) of some systems under investigation: 1-DNA; 2-*meso*-tri(*N*-methyl-4-pyridinium)porphyrinyl-*p*-phenylene-5'-*O*-thymidine; PT, 3- DNA-PT; 4-*meso*-tetra(*N*-methyl-4-pyridinium)porphyrin, tpyP; 5- DNA-tpyP.

notions should be considered based on the 240-220 nm region. This region is devoid of any maxima in the experimental spectra of T and A alone and in the spectrum of the T···A pair. The calculations suggest only the appearance of bands of very small intensity for this region. However, when T becomes attached to P, a clear maximum in that region of the experimental spectrum appears (at 255 nm). The interaction with A, PT···A, like the interaction of DNA-PT with A, also results in new bands which are visible as shoulders on other peaks. The attachment of A to DNA-PT, (DNA-PT···A), results in greater blue-shift than attachment to PT, (PT···A)(shifts to 229 nm and 223 nm *vs* 235 nm and 224 nm for the two types of attachment). Characteristically for the DNA-PT system alone, nothing comparable to that could be seen. It is interesting that the calculated values for the *ca* 260 nm region resulting from the qPT → qPT···A (**4** → **5**) transformations correspond quite well to the experimental changes accompanying the PT → DNA-PT → DNA-PT···A, and PT → PT···A transformations. For the 240-220 nm region, calculations for both T and qPT point to the absorption at *ca* 233 nm, which as the result of interaction with A, (qPT···A), is shifted to 231-228 nm. Since in the experimental spectra absorption rises intensively toward the 200-190 nm region, the small maxima in question are mostly buried there and appear only as slightly marked shoulders at 226 nm in the case of PT. Those are not visible for DNA-PT or for T···A, however, they become again slightly marked for PT···A and DNA-PT···A systems in the 229-223 nm range. This means that although attachment of A does not cause the alteration of the experimental spectra as is suggested by calculations, it increases the intensity enough to make the shoulders visible. This is not a case for systems in which A is absent.

The above discussed results suggest that, when changes observed in the uv-vis spectra and sterical factors are considered, there is no reason why interactions should not take place between porphyrinyl-thymidine and porphyrinyl-adenosine, (PT···AP), when both porphyrin units are already interacting with different DNA molecules. There are, however, reasons to not overestimate the role of intercalation in the phenomenon of attachment to DNA of porphyrin units of each participating porphyrinyl-nucleoside.

Additional support for that option was expected from the investigation of the interaction with DNA of immobilized porphyrin (compare [9,10], in which the *meso*-tri(*N*-methylpyridinium)porphyrin units are the same as in PT. With immobilized porphyrin, the porphyrin units attached to the solid silica support *via* propylamide bridges, Figure 11, should not have enough conformational flexibility to intercalate effectively into ds DNA. Additional restriction arises from the aminopropyl groups attached to the support, which remained uninvolved in the formation of covalent amide bonds with porphyrin (for the latter purpose, porphyrin had to contain *p*-carboxyphenyl *meso*-substituent before its attachment to the solid support). In spite of these limitations, the immobilized porphyrin interacted with ds DNA decreasing its concentration. Unfortunately, due to the presence of a strong band at about 230 nm arising from the amide bond, the 260 nm band used to measure the changes in concentration of DNA in solution, appeared as a shoulder which made it difficult to determine quantitative conclusions. Characteristically, though,

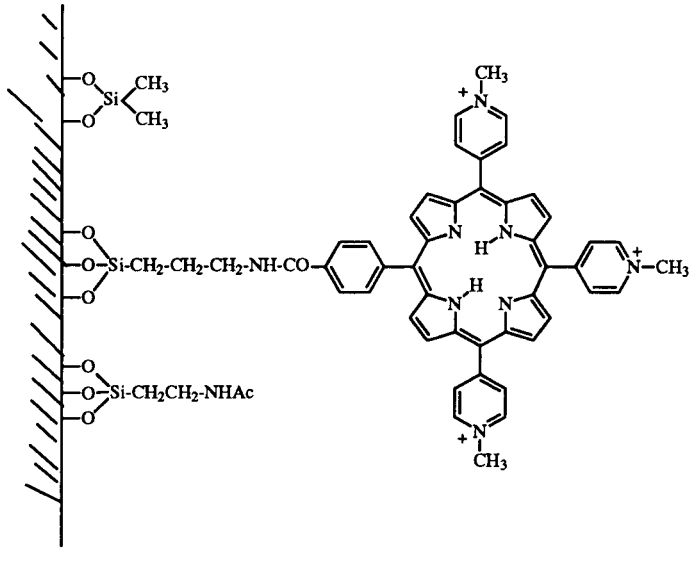

Figure 11. Immobilized cationic porphyrin used for interaction with DNA.

the respective immobilized porphyrin containing the non-cationic pyridyl substituents did not remove DNA from the solution to a meaningful extend.

Theoretical.

All calculations were performed with HyperChem 4.0 (Hypercube Inc., Waterloo, Ontario Canada) on a Pentium computer. Initial starting geometries for the conformational analyses were generated using the MMX force field [2] within PCMODEL [11], fixing torsional angle 4-3-2-1 (see Figure 2) at the values of 180° and 75° for additional computations. At each of these orientations of the side chain, rotations of the C_6H_5-O-CH_2 group were examined by simultaneously driving torsional angle 6-5-4-3 from -90° to 90° in 15° increments and torsional angle 5-4-3-2 from 0° to 360° in 15° increments. The potential energy *vs* conformation surfaces indicated the presence of 7 and 6 local maxima, for *p*-phenyl-5'*O*-thymidine and -adenosine, respectively, which were then twice optimized by the AM1 semi-empirical method [3] within MOPAC 6.0 [12], utilizing the molecular mechanics correction for amide bonds. Two of the molecular mechanics-generated structures were optimized to the same geometry by AM1. In calculation of the porphyrinyl-nucleoside dimer, qPT···APq, each half was assembled as follows. An optimized structure for *meso*-pyridylporphyrin was joined to a pre-optimized structure of the nucleoside. On the thimidine side of the dimer the torsional angles considered were 6-5-4-3 = -3°, 5-4-3-2 = -79° and 4-3-2-1 = -54°. The respective angles considered on the adenine side were -8°, -72° and -55°. This structure was completely optimized, the appropriate Ph-O-CH_2 torsional angles form the preferred conformer of each half-dimer imposed on the phenyl-nucleoside linkage, and the structure optimized. The optimized half-structures were then brought together in an approximate geometry that formed the specific hydrogen bonding pattern. The dimer was initially optimized with the N-H-O and the N-H-N distances fixed at 2.1 Å and 3.3 Å, respectively. These distance constraints were removed for the final MMX geometry optimization.

The uv-vis spectral lines were predicted for the selected structures by single point 6 x 6 configuration interaction CI calculations on the optimized geometry. For each structure, the pyridine (or protonated pyridinium) substituent was then rotated to be co-planar or angled (at 70°) with the porphyrin ring, and without geometry optimization, the single-point 6 x 6 CI AM 1 calculation was repeated.

EXPERIMENTAL

The following commercially available chemicals from Aldrich (unless otherwise stated) were used without further purification; adenine, adenosine, *meso*-tetra-4-pyridylporphyrin, sodium hydride as 60% suspension in mineral oil, cesium carbonate, *p*-anisaldehyde, *p*-carboxybenzaldehyde, 4-pyridinecarboxaldehyde, pyrrole, propionic acid, dichlorodimethylsilane, iodomethane, nitomethane, pyridine, acetic anhydride, triethylamine, *N,N*-dimethylformamide, absolute ethanol (Quantum Chemical), chloroform (Baker), methanol (Baker), dichloromethane (Baker), 3-aminopropylsilica gel, silica gel 70-230 mesh 60 Å, and the sheets with silica gel 60 F_{254} (EM Reagents). Plasmid DNA was purified using the Wizard Fast MaxiPrep Kit obtained from Promego, Inc. (Madison, WI). All restriction endonuclease enzymes were obtained from USB, Inc. (Cleveland, OH).

Atom bombardment mass spectrometry was performed on a V6 Micromass 70/70 mass spectrometer with an 11/250 data system, 3-nitrobenzyl alcohol applied as a matrix. The ^{1}H nmr spectra were recorded on a Bruker IBM AF 300 MHz Fourier transform spectrometer. Electronic absorption spectra were recorded on a Perkin-Elmer Lambda 4C uv-vis spectrometer model C 688-0002 and Hewlett-Packard 8452A Diode Array spectrophotometer.

meso-5,10,15-Tri-4-pyridyl-20-(*p*-phenylene-5'-*O*-thymidine)-porphyrin **1**.

A solution of *meso* 5,10,15-tri-4-pyridyl-20-*p*-hydroxphenyl-porphyrin, obtained as described by us in [1], (150 mg, 0.24 mmole) and 5'-*O*-tosylthymidine [13] (188 mg, 0.48 mmole) in *N,N*-dimethylformamide (100 ml) was added dropwise over a period of 2 hours at 65° to a solution of sodium hydride (60%) (58 mg, 1.44 mmoles) and cesium carbonate (78 mg, 0.24 mmole) in *N,N*-dimethylformamide (100 ml). After stirring at that temperature for 48 hours, the mixture was cooled to room temperature and filtered. The filtrate was added to water (300 ml) and methanol (100 ml) and extracted with chloroform (3 x 50 ml). The combined chloroform layers were washed with 5% aqueous ammonia, then with water and dried over anhydrous sodium sulfate. After evaporation of the solvent, the residue was chromatographed on a silica gel column, chloroform/methanol 20:1 as an eluent. Product **1** (21 mg) appeared as the second fraction, yield 10%; ms: fab (m/z) $(M+1)^+$ 858; ^{1}H nmr (deuteriodimethyl sufoxide): 11.41 (s, 1H N[3]H), 9.04 (d, 5.0 Hz, 6H py), 8.89 (s, β-pyr), 8.26 (d, 4.7 Hz, 6H py), 8.15 and 7.44 (dd, 7.9 Hz, 4H phen), 7.71 (s, 1H, H-6), 6.40-6.33 (m, 1H, H-1'), 5.59 (d, 4.1 Hz, 1H, H-3'), 4.57-4.28 (m, 3H, H-4', H-5', H-5"), 2.29 (m, 2H, H-2',2"), 1.84 (s, 3H, C-5-CH_3), -3.00 (s, 2H, NH por); uv-vis (chloform/methanol 1:1): λ (nm) 196, 226, 266, 413 (S), 510, 548.5, 572, 634.

Anal. Calcd. for $C_{51}H_{39}N_9O_5$: C, 71.39; H, 4.58; N, 14.69. Found: C, 71.28; H, 4.52; N, 14.85.

meso-5,10,15-tri(*N*-methyl-4-pyridinium)-20-(5'-*O*-thymidine)-porphyrin, Iodide Salt **2** (PT).

Compound **1** (15 mg, 0.017 mmole) and iodomethane (4 ml) in 5 ml of nitromethane were mixed and refluxed at 50° for 12 hours. The nitromethane and excess iodomethane were removed under high vacuum to give 20 mg of product; yield, 94%; ^{1}H nmr (deuteriodimethyl sufoxide): 11.44 (1H N[3]H), 9.50 (d, 6.5 Hz, 6H py), 9.18 (m, 2H py), 9.07-9.00 (11H, 3H py, 8H β-pyr), 8.20 and 7.53 (dd, 8.5 Hz, 4H phen), 7.74 (s, 1H, H-6), 6.39 (t, 1H, H-1'), 5.60 (m, 1H, H-3'), 4.74 (s, 9H, N-CH_3), 4.57 and 4.32 (m, 3H, H-4', H-5', H-5"), 2.33 (m, 2H, H-2'), 1.86 (s, 3H C-5-CH_3), -2.99 (s, 2H, NH por); uv-vis (water): λ (nm) 223, 261, 426 (S), 521, 585, 643.

Anal. Calcd. for $C_{54}H_{48}N_9O_5I_3$: C, 50.52; H, 3.77; N, 9.82. Found: C, 50.28; H, 3.91; N, 10.01.

meso-Tri(*N*-methyl-4-pyridinium)-20-*p*-carboxyphenylporphyrin immobilized on 3-Aminopropylsilica gel **3**.

To refluxing propionic acid (750 ml) 4-pyridinealdehyde (14.3 ml, 0.15 mmole) and *p*-carboxybenzaldehyde (7.5 g, 0.05 ml) were added. Once the aldehydes were completely dissolved, freshly distilled pyrrole (13.9 ml, 0.2 mole) was added and refluxing was continued for 1 hour. The volume of solvent was reduced to 50 ml under reduced pressure. The mixture was then neutralized with sodium bicarbonate solution, filtered and washed several times with water. The crude product was allowed to air-dry and then purified twice by silica gel column chromatography using chloroform/methanol 25:1 as eluent, yield 5%; fab ms spectrum showed $(M+1)^+$ 663 m/z. This porphyrin derivative (20 mg, 0.031 mmole) was dissolved in dichloromethane (35ml) at 15-20° and 1,1'-carbonyldiimidazole (5.0 mg, 0.031 mmole) was added. The reaction mixture was stirred overnight under nitrogen. Then, it was diluted to 20 ml with dichloromethane and 3-aminopropylsilica gel (120 mg), which contained 10.6% of hydroxy groups functionalized by aminopropyl groups, was added and sonication carried out for 8 hours. The precipitate was filtered and washed with chloroform, chloroform/methanol and then methanol until washings were colorless. The product obtained was dried under high vacuum, the yield of the immobilized *meso*-tri-4-pyridyl *p*-phenylene-amidopropylporphyrin obtained was 110 mg, 67%, as indicated by elemental analysis. A portion of the immobilized porphyrin (50 mg) was refluxed with acetic anhydride (5 ml) in triethylamine for 2.5 hours. The solvent was then pumped off under high vacuum and the residue refluxed with dichlorodimethylsilane (5 ml) to block the free hydroxyl groups. The excess dichlorodimethylsilane was rotavaped and the residue washed with 10% solution of triethylamine in diethyl ether. The product (28 mg), containing porphyrin units in the form of the *meso*-tri-4-pyridyl derivatives, was refluxed with iodomethane (1 ml) and nitromethane (1 ml) overnight and thoroughly washed with chloroform. The yield of the immobilized *N*-methyl-4-pyridinium derivative **3** was 21 mg.

DNA Testing.

The plasmid pRIT **5** was isolated from *E. coli* harboring the plasmid using the Wizard MaxiPrep Kit. The protocol provided by the manufacturer was followed exactly. The plasmid was verified to be correct by restriction endonuclease digestion and analysis of fragment sizes. Agarose gel electrophoresis and ethidium bromide staining were used to visualize the DNA. The uncut plasmid was 6800 base pairs.

pRIT **5** was restricted with *E. coli* enzyme which cleaved the DNA at a unique site resulting in linear DNA. DNA (25 µg, 15 ml), 10 x RE buffer (3 µl), water (11 µl) and EcoR1 enzyme (1 µl) were incubated at 37° for 3 hours. The restriction enzyme was removed from the DNA solution by reacting with phenol (1/2 volume) followed by chloroform (1.5 volume). The aqueous phase containing the DNA was removed to a new tube, sodium acetate was added to a final concentration of 0.3 mole and the DNA was precipitated with two volumes of ice cold 100% ethanol. The DNA pellet was resuspended in 200 µl water. Known concentration of porphyrin was added to a known concentration of DNA and they were incubated for 5 minutes after which their absorbance was read on a uv spectrophotometer.

To study the interaction of water soluble porphyrin derivatives with DNA, stock solutions used were as follows: DNA 1.7 µg/µl, compound **2** (PT) 1 µg/µl, adenine and adenosine were both at concentrations 2.5 µl/µl. Ultraviolet-vis readings were taken by adding 1-5 µl of DNA to 1-10 µl compound **2** and/or thymidine, adenine or adenosine. This was diluted to a final volume of 600 µl with water before taking the uv-vis measurements. In these experiments DNA was not cleaved.

To study interaction of DNA with immobilized porphyrin, three samples were used: (a) *meso*-tri(*N*-methyl-4-pyridinium)porphyrin attached to aminopropylsilica gel as shown in Figure 11, compound **3**; (b) respective non-*N*-methylated material, and (c) 3-aminopropylsilica gel. Each sample (0.20 mg) was packed into a separate 3 ml biorad disposable column. The samples were washed thoroughly with TE buffer (10 mmoles Tris, 1 mmole EDTA, *p*H 8.0) until the OD at 260 nm was close to zero. At this point DNA solution in water (1.7 µl/µl) was added to each column and collected 1 ml fractions. Then the OD was determined at 260 nm. The DNA had been quantified to determine the amount bound to the column by calculating how much was removed from the starting material.

Acknowledgments.

We are thankful to the State Board of Education in Boise for supporting this research with a Special Research Grant, and to Idaho EPSCoR for a Mini-grant. We also thank Dr. Michael Sherrod for the computational work.

REFERENCES AND NOTES

[1] L. Czuchajowski, J. Habdas, H. Niedbala and V. Wandrekar, *J. Heterocyclic Chem.*, **29**, 479 (1992).

[2] J. J. Gajewski and K. E. Gilbert, Adv. Mol. Modeling, **2**, 65 (1990).

[3] M. J. S. Dewar, E. G. Zoebisch, E. F. Healy and J. J. P. Stewart, *J. Am. Chem. Soc.*, **107**, 3902 (1985).

[4] A. A. Tulub, Opt. Sapektrosk., **68**, 1031 (1990).

[5] K. Butje, J. H. Schneider, J. P. Kim, Y. Wang, S. Ikuta and K. Nakamoto, *J. Inorg. Biochem.*, **37**, 119 (1989).

[6] R. F. Pasternak, E. J. Gibbs and J. J. Villafranca, *Biochemistry*, **22**, 2406 (1983).

[7] L. Czuchajowski, J. E. Bennett, S. Goszczynski, D. E. Wheeler, A. K. Wisor and T. Malinski, *J. Am. Chem. Soc.*, **111**, 607 (1989).

[8] R. R. Monaco and M. Zhao, *Int. J. Quant. Chem.*, **46**, 701 (1993).

[9] C. E. Kibbey and M. E. Meyerhoff, *Anal. Chem.*, **65**, 2189 (1993).

[10] B. L. Iverson, R. E. Thomas, V. Kral and J. L. Sessler, *J. Am. Chem. Soc.*, **116**, 2663 (1994).

[11] P. C. Model Version 4.0 for DOS. Serena Software, Bloomington, IN.

[12] MOPAC 6.0, QCPE Program 504. DOS version. Serena Software, Bloomington, IN.

[13] E. I. Reift, A. Benitez and L. Goodman. *J. Org. Chem.*, **29**, 554 (1964).